Phase-dependent deterministic switching of magnetoelectric spin wave detector in the presence of thermal noise via compensation of demagnetization

Article *in* Applied Physics Letters · November 2015

DOI: 10.1063/1.4935690

5 authors, including:

Sourav Dutta
Georgia Institute of Technology

Dmitri Evgenievich Nikonov
Intel

Phase-dependent deterministic switching of magnetoelectric spin wave detector in the presence of thermal noise via compensation of demagnetization

Sourav Dutta,[1, a)] Dmitri E. Nikonov,[2] Sasikanth Manipatruni,[2] Ian A. Young,[2] and Azad Naeemi[1]
[1)] *School of Electrical and Computer Engineering, Georgia Institute of Technology, Atlanta, GA 30332 USA.*
[2)] *Components Research, Intel Corporation, Hillsboro, OR 97124 USA.*

The possibility of achieving phase-dependent deterministic switching of the magnetoelectric spin wave detector in the presence of thermal noise has been discussed. The proposed idea relies on the modification of the energy landscape by partially canceling the out-of-plane demagnetizing field and the resultant change in the intrinsic magnetization dynamics to drive the nanomagnet towards a preferential final magnetization state. The remarkable increase in the probability of successful switching can be accounted for by the shift in the location of the saddle point in the energy landscape and a resultant change in the nature of the relaxation dynamics of the magnetization from a highly precessional to a fairly damped one and an increased dependence on the initial magnetization values, a crucial requirement for phase-dependent spin wave detection.

For more than four decades, the complementary metal-oxide-semiconductor (CMOS) integrated circuits has had an unprecedented success from scaling its dimensions with each technology generation, resulting in an exponential growth and around 8 orders of magnitude improvement in the performance. However, the recent projections by International Technology Roadmap for Semiconductors (ITRS) suggest the apparent conclusion of the scaling trend due to fundamental physical limitations of device switching[1–3]. This has lead to an aggressive global research thrust for finding alternative devices and state variables for beyond-CMOS device technology. Electron spin, as a computational state variable for logic devices and circuits, has been the focus of active research[1–5]. Among the various members in the spintronics family, the possibility of utilizing spin waves for information transmission and computation has been an area of active research due to the unique ability to manipulate the amplitude and phase of the spin waves for building complex logic circuits with less physical resources and low power consumption[6–11]. Some of the previous proposals on spin wave logic circuits have suggested the idea of utilizing the magnetoelectric (ME) effect for efficient spin wave generation, amplification and amplitude- or phase-dependent switching of the magnetoelectric cell[8–12].

Recently, a comprehensive scheme for building a clocked non-volatile spin wave device has been suggested that satisfies the five essential requirements for logic application: nonlinearity, amplification, concatenability, feedback prevention, and complete set of Boolean operations[13]. The underlying working principle is to utilize the ME effect to create a voltage-induced in-plane isotropic strain in the piezoelectric layer that gets coupled to the adjacent ferromagnetic layer of the ME cell, creating a strain-induced out-of-plane magnetic anisotropy. Above a critical strain, the magnetic easy-axis rotates out-of-plane causing an out-of-plane switching of magnetization and creating spin waves. Once out-of-plane, the magnetization continues to be held in the meta-stable state via application of voltage until the incoming propagating spin wave signal reaches the ME cell. Upon arrival, the voltage is turned off, causing the magnetization to relax back to the in-plane configuration with initial magnetization angles $\theta = cos^{-1} mz$ and $\phi = tan^{-1} \frac{my}{mx}$ provided by the phase of the spin wave. Once in-plane, the magnetization continues to store the information bit in a stable magnetic state (non-volatile memory).

While the effect of thermal noise is to introduce random fluctuations to the internal anisotropic field[14,15] and thus affect the magnetization dynamics of the ME cell, the impact is most critical during the course of detection of the spin wave. The effect is twofold: (i) randomizing the phase of the arriving spin wave, ie, fluctuations in the value of the initial magnetization angles θ and ϕ provided by the spin wave, and (ii) affecting the trajectory of the magnetization relaxation dynamics from out-of-plane to in-plane configuration. It is seen that even if the fluctuation in the initial angles are minimized, a small variation in the trajectory of the magnetization can have a significant effect on the final magnetic state, making the switching non-deterministic. In this work, we focus on minimizing the variation of the magnetization relaxation trajectory by modifying the energy landscape of the ME cell. Such a modification is realized by utilizing the concept of compensation of demagnetization field[16]. A noticeable increase in the switching success is seen showing a remarkable impact of the compensation of demagnetization. The rest of the paper is as follows- in the first half, we use a simple macrospin model to demonstrate the impact of partially canceling the demagnetizing field on the deterministic switching of the magnet. Then we implement the idea in our previously proposed clocked non-volatile spin wave device[13], showing a major improvement in the reliability of the spin wave detector in the presence of thermal noise.

We start by analyzing an isolated nanomagnet in the

[a)] Electronic mail: sdutta38@gatech.edu

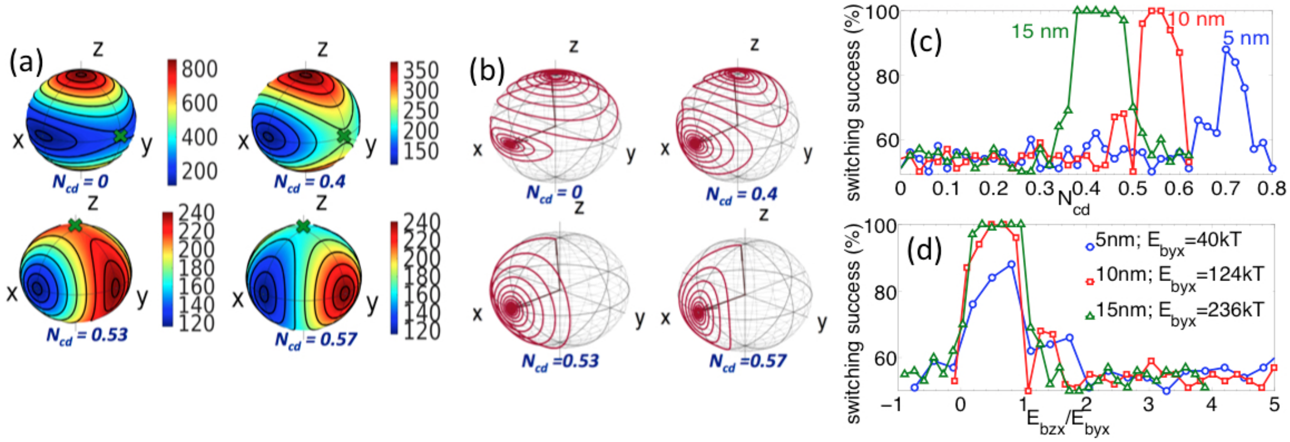

FIG. 1: (a) Energy landscape of a 80 nm × 40 nm × 10 nm nanomagnet for different compensation of demagnetization (colormap shows energy in kT). The blue and red regions denote the energy minima and maxima respectively. The green "X" represents the saddle point. The black lines represent the constant energy trajectories in which the magnetization gyrates in the absence of damping and thermal noise.(b) Magnetization trajectories as it relaxes from out-of-plane meta-stable state (z) to stable in-plane (±x) configuration. (c) Switching success of the nanomagnet as a function of compensation of demagnetization for 5, 10 and 15 nm thickness. The lateral dimensions are kept constant at 80 nm × 40 nm. (d) Switching success as a function of the ratio of the energy barriers E_{bzx}/E_{byx}.

shape of a cuboid with x, y and z being the in-plane easy axis, in-plane hard axis and out-of-plane hard axis respectively, using a simple macrospin model. The scenario of spin wave detection, where the ME cell is allowed to relax from an out-of-plane metastable to an in-plane stable state with initial magnetization angles θ and ϕ provided by the spin wave, is mimicked by allowing the magnetization of the nanomagnet to fall in-plane from an initial out-of-plane state with fixed $\theta = 5°$ and $\phi = 0°$. The choice for the initial angles is in close agreement with that provided by spin waves. We neglect the fluctuations in the angles since we focus only on the relaxation dynamics under thermal noise. The stochastic Landau-Lifshitz-Gilbert (sLLG) equation describing the dynamics of the nanomagnet in the presence of thermal noise can be written as

$$\frac{d\hat{m}}{dt} = -\gamma\mu_0\left[\hat{m}\times\vec{H}_{eff}\right] + \alpha\left[\hat{m}\times\frac{d\hat{m}}{dt}\right] \quad (1)$$

where $\hat{m} = \vec{M}/M_s$ is the unit magnetization vector, M_s is the saturation magnetization, γ is the gyromagnetic ratio, α is the Gilbert damping parameter and $\vec{H}_{eff} = \vec{H}_d + \vec{H}_t + \vec{H}_{cd}$ is the effective internal magnetic field, including shape anisotropy and thermal noise. The shape anisotropy or the demagnetizing field is given by $\vec{H}_d = -M_s\left(N_x\hat{m}_x + N_y\hat{m}_y + N_z\hat{m}_z\right)$, where N_x, N_y and N_z are the demagnetization tensors depending on the geometry of the magnet[17]. At room temperature T, a Gaussian white noise is used to model the thermal field, acting isotropically on the nanomagnet[15] and written as

$$\vec{H}_t = H_x\hat{x} + H_y\hat{y} + H_z\hat{z} \quad (2)$$

$$= \sqrt{\frac{2\alpha k_B T}{\mu_0^2\gamma M_s V}}\left(\frac{\partial W_x}{\partial t}\hat{x} + \frac{\partial W_y}{\partial t}\hat{y} + \frac{\partial W_z}{\partial t}\hat{z}\right) \quad (3)$$

where V is the volume of the nanomagnet and W_x, W_y and W_z are the three independent Wiener process in x, y and z directions respectively. The internal field satisfies the following conditions:

$$< H_i(t) > = 0 \quad (4)$$

$$< H_i(t)H_j(t') > = \frac{2\alpha k_B T}{\mu_0^2\gamma M_s V}\delta(t-t')\delta_{ij} \quad (5)$$

As indicated by Liu et al.[16], the compensation in out-of-plane demagnetizing field can be achieved by utilization of Co/Ni multilayers. The out-of-plane magnetic anisotropy $K_\perp$ arising from the Co/Ni interfaces can be tuned over a wide range by changing the thickness of each layer and/or the number of repeats[18]. It has been demonstrated that with the right thickness and repeats, one can achieve the desired condition of a reduced demagnetizing field. Alternatively, one can achieve a similar compensation of demagnetizing field and hence, tune the out-of-plane tilting of an in-plane magnetized ferromagnetic film (say, nickel or permalloy) coupled with a strong PMA material (say, [Co/Pd]) by varying the thickness of the ferromagnetic layer[19]. However, here we avoid such complications by simply adding an additional anisotropy term

$$\vec{H}_{cd} = \frac{2K_\perp}{\mu_0 M_s}\hat{m}_z = N_{cd} M_s \hat{m}_z \tag{6}$$

to $\vec{H}_{eff}$ to account for the compensation in the out-of-plane demagnetizing field, the degree of compensation being denoted by N_{cd}. The sLLG equation (1) is solved using mid-point method in the sense of Stratonovich calculus[20].

In the absence of damping and thermal noise, the magnetization does precessional rotation in a conservative or constant energy trajectory which can be distinguished into two categories - high energy orbit around the out-of-plane hard axis (z), also called "out-of-plane precession (OPP)" and low energy orbit around the in-plane easy axis (x), also called "in-plane precession (IPP)". The evolution of such trajectories can be described analytically by solving the LLG equation in the absence of damping and thermal noise[21,22]. The energy landscape of the nanomagnet and a set of such constant energy trajectories under no compensation ($N_{cd} = 0$) are shown in Figure 1 (a). Note the positions of the energy minina, saddle point (marked by "X") and energy maxima, which are along the x ,y and z-axis respectively. Upon adding the contribution of damping, the dynamical evolution of the magnetization deviate from the constant energy trajectory and the closed orbit transforms into a finely spiraling trajectory approaching an energy minima as illustrated in Figure 1(b) with $N_{cd} = 0$. The magnetization follows the constant energy trajectories fairly closely, drifting slowly from one higher energy trajectory to the next lower one, losing energy in the process via damping. Note the large number of precessional rotations the nanomagnet has to make before it can come down to one of the energy minima ($\pm x$ state). Such a trajectory is highly vulnerable to thermal noise and even a small deviation in the magnetization path can make it fall to either of the energy minima, making the switching process non-deterministic.

However, one can imagine a case where the energy landscape of the nanomagnet is modified by lowering the out-of-plane energy barrier $E_{bzx} = \frac{1}{2}\mu_0 M_s^2(N_z - N_{cd} - N_x)V$ via a small compensation N_{cd}. This alters the constant energy orbits, lowering the number of OPPs and making more concentric IPPs around the energy minima (Figure 1 (a) with $N_{cd} = 0.4$). However, the nanomagnet still has to do precessional rotations around the z-axis in-order to fall to one of the energy minima as shown in Figure 1(b) with $N_{cd} = 0.4$. Beyond a critical compensation $N_{cd} = (N_z - N_y)$, E_{bzx} becomes lower than the in-plane energy barrier $E_{byx} = \frac{1}{2}\mu_0 M_s^2(N_y - N_x)V$ and the saddle point shifts to the z axis while the y-axis becomes the energy maxima. The energy landscape and a set of constant energy trajectories under this scenario is shown in Figure 1 (a) with $N_{cd} = 0.53$ and 0.57. Consequently, the dynamical evolution of the magnetization changes from a highly precessional one to a fairly damped one as shown in Figure 1 (b) with $N_{cd} = 0.53$ and 0.57. The cut down in the precessional trajectories makes the relaxation of the magnetization primarily dependent on the initial magnetization angle (θ and ϕ), with very little scope for the thermal fluctuations to alter the path of the magnetization and make the switching non-deterministic. It must be noted that there are two constraints which limit the degree of compensation. Firstly, beyond a threshold value $N_{cd} = (N_z - N_x)$, E_{bzx} becomes negative, denoting that the in-plane stable magnetization states ($\pm x$) are lost and the magnet becomes perpendicularly magnetized even in the absence of any ME effect. Secondly, the energy barrier E_{bzx} decreases with the increase in compensation N_{cd} and beyond a certain threshold, crosses the 40 kT mark, a minimum required for retaining any reasonable memory state lifetime. Finally, we test for the impact of compensation of demagnetization on the switching success of the nanomagnet by performing numerical simulations in the presence of thermal noise. We take Ni as the nanomagnet material and perform 100 simulations for each of the data points to capture the effect of thermal noise. With the initial magnetization angle fixed at $\theta = 5°$ and $\phi = 0°$, we define the switching success as the probability of the nanomagnet to fall into a preferred final magnetization state, ie, either +x or -x. Figure 1 (c) shows the remarkable impact of compensation of demagnetization on the switching success of the nanomagnet, paving the path for a more thermally reliable spin wave device. The sharply defined window where the switching success drastically increases can be obtained when the ratio $E_{bzx}/E_{byx} < 1$ as shown in Figure 1 (d) and is given by

$$\Delta \le E_{bzx} \le E_{byx} \tag{7}$$

$$N_z - N_y \le N_{cd} \le N_z - N_x - \frac{2\Delta}{\mu_0 M_s^2 V} \tag{8}$$

where $\Delta \sim 40kT$. Note that for 5 nm thickness, even if the saddle point shifts to z axis under the condition $E_{bzx}/E_{yx} < 1$, the switching success is still low which maybe the result of a relatively low energy barrier $E_{byx} \sim 40kT$ or a relatively small volume of the nanomagnet.

Next we investigate the impact of compensation of demagnetization in a single-stage clocked spin wave device consisting of a transmitter ME cell (ME1), a detector ME cell (ME2) and spin wave interconnects as shown in Figure 2(a). The operating principle has been described earlier and a more detailed description is given in Ref. [13]. As mentioned earlier, we introduce the compensation of demagnetization field as an additional perpendicular magnetic anisotropy $K_\perp$ term applied only to the ME cell. We perform 1-D micromagnetic simulations using the Object Oriented Micromagnetic Framework (OOMMF)[23] that numerically solves the stochastic Landau-Lifshitz-Gilbert (sLLG) equation augmented with thermal noise. We choose Ni/PZN-PT heterostructure for the ME cell and [Co/Ni] multilayer with reduced PMA and saturation magnetization for the SWB to minimize the attenuation of the spin waves. The material parameters used are summarized in Table I. We repeat

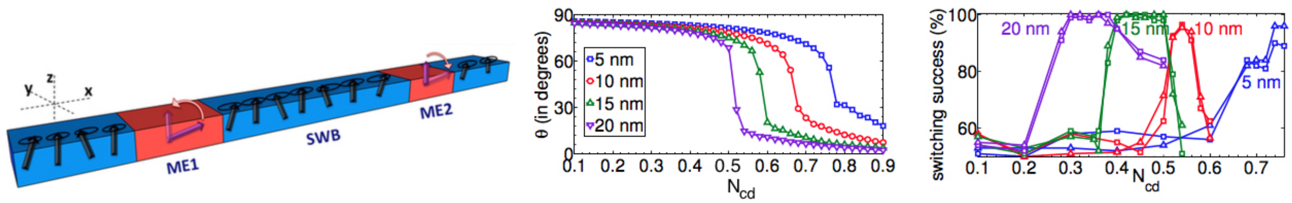

(a) (b) (c)

FIG. 2: (a) Schematic of a single-stage clocked spin wave device. (b) Out-of-plane magnetization tilt angle $\theta = cos^{-1}mz$ of the ME cell as a function of the compensation of demagnetizing field. (c) Impact of the compensation of demagnetization on the switching success of the spin wave detector. The symbols square and triangle represent the case when bit 1 and 0 are transmitted respectively.

each simulation 100 times in order to capture the effect of random thermal noise.

The partial cancellation of the out-of-plane demagnetizing field tends to reduce the in-plane stability of the magnetization by modifying the energy landscape and lowering the energy barrier E_{bzx}. Due to the competition between the shape anisotropy and the small perpendicular magnetic anisotropy $K_\perp$ of the ferromagnetic layer of the ME cell (compensating the demagnetizing field), unique magnetic configurations can be achieved. We first explore the out-of-plane magnetization tilt angle $\theta = cos^{-1}mz$ of the ME cell. Figure 2(b) shows that the tilt angle is highly tunable over a range of compensation of demagnetization. Ensuring that the tilt angle is within a reasonable range that allows us to have atleast a 40 kT energy barrier E_{bzx}, we vary the compensation and calculate the probability of achieving a deterministic switching of magnetization via spin waves. We see an appreciable increase in the switching success showing a remarkable impact of the compensation of demagnetization. It must be noted that despite the addition of numerous other contributions like the exchange interactions within the ME cell and between the ME cell and adjacent SWB, or the complicated nature of demagnetization field in this micromagnetic problem, the underlying physics, ie., the shift of the saddle point in energy landscape and change in the constant energy orbits, remains the same. However, unlike the investigation with the simple macrospin model where we assumed a fixed θ and ϕ, here, depending on the time of clocking of ME2, ie, the instance at which the voltage is turned off, we may end up with different values of θ and ϕ provided by the incoming spin wave for the same input (say, transmission of bit 1) which may vary the result slightly. However, the overall trend of the switching success remains the same. Also note that due to thermal noise, for the same instance of clocking of ME2, the initial magnetization angles θ and ϕ provided by the spin wave bus fluctuates which may result in some failure cases and restrains the detector from achieving a 100% switching success. We believe this fluctuation in the angles can be reduced via the appropriate choice of material parameters and dimensions and can be the focus of a future work.

An added advantage of the compensation in demagnetization is that due to the lowering of the out-of-plane energy barrier E_{bzx}, the magnetostriction needs to change anisotropy by a smaller amount, maybe $\sim 100kT$ rather than $\sim 600kT$ to switch a transmitter or receiver ME cell between in-plane and out-of-plane states. This drastically brings down the voltage required to create the strain and hence the power dissipation. Our simulations revealed that a minimum of $0.26V$ is required for out-of-plane switching of 15 nm thick ME transmitter when there is no compensation, resulting in an energy dissipation of $E = \epsilon_0\epsilon_r A_{ME}V^2/2t_{PZ} = 32aJ$. The minimum required voltage goes down to $0.06V$ for $N_{cd} = 0.5$ reducing the energy dissipation by 16 times.

TABLE I: Material parameters

Parameter	Value
Length of ME cell	80 nm
Length of SWB	100 nm
Width	40 nm
Thickness	5-20 nm
Saturation magnetization Ms	500 kA/m
Exchange constant A_{exch}	9 pJ/m
Gilbert damping constant for ME cell	0.05
Gilbert damping constant for SWB	0.01
Perpendicular anisotropy of SWB K_{SWB}	158 kJ/m^3
Magnetostrictive coefficient λ	-32.9 ppm[24]
Young's modulus Y	214 GPa[25]
Piezoelectric coefficient d_{31}	1100 pm/V[24]
Dielectric constant of piezoelectric layer ϵ_r	1000
Thickness of piezoelectric layer t_{PE}	30 nm

In conclusion, we have theoretically demonstrated the possibility of achieving phase-dependent deterministic switching of the magnetoelectric spin wave detector in the presence of thermal noise. The proposed idea is based on modifying the energy landscape of the ME cell by partially canceling the out-of-plane demagnetizing field. This results in a shift of the saddle point from the in-plane hard axis to the out-of-plane hard axis. The metastable state of the ME cell now being closer to the saddle point, the magnetization undergoes a damped relaxation dynamics instead of a highly precessional one. This drives the detector ME cell towards a preferential final magnetization state, depending primarily on the initial magnetization values, a crucial requirement for phase-dependent spin wave detection. We believe any additional reduction in the thermal fluctuation of the detected phase of the spin wave in conjunction with this work can lead to further improvement of the switching probability. The proposed concept of utilizing the compensation of demagnetizing field can be easily realized by using a PMA baselayer underneath the ferromagnetic layer of ME cell or the PMA SWB underneath the ME cell to achieve a tunable tilting of magnetization and a resultant compensation.

[1] D. E. Nikonov and I. A. Young, "Overview of beyond-cmos devices and a uniform methodology for their benchmarking," Proceedings of the IEEE **101**, 2498–2533 (2013).

[2] K. Bernstein, R. K. Cavin, W. Porod, A. Seabaugh, and J. Welser, "Device and architecture outlook for beyond cmos switches," Proceedings of the IEEE **98**, 2169–2184 (2010).

[3] J. Kim, A. Paul, P. Crowell, S. J. Koester, S. S. Sapatnekar, J.-P. Wang, and C. H. Kim, "Spin-based computing: Device concepts, current status, and a case study on a high-performance microprocessor," Proceedings of the IEEE **103**, 106–130 (2015).

[4] S. A. Wolf, D. D. Awschalom, R. A. Buhrman, J. M. Daughton, S. von Molnr, M. L. Roukes, A. Y. Chtchelkanova, and D. M. Treger, "Spintronics: A spin-based electronics vision for the future," Science **294**, 1488–1495 (2001).

[5] S. A. Wolf, J. Lu, M. R. Stan, E. Chen, and D. M. Treger, "The promise of nanomagnetics and spintronics for future logic and universal memory," Proceedings of the IEEE **98**, 2155–2168 (2010).

[6] A. Khitun and K. L. Wang, "Nano scale computational architectures with spin wave bus," Superlattices and Microstructures **38**, 184–200 (2005).

[7] A. Khitun, M. Bao, and K. L. Wang, "Magnonic logic circuits," Journal of Physics D: Applied Physics **43**, 264005 (2010).

[8] J. Alzate, P. Upadhyaya, M. Lewis, J. Nath, Y. Lin, K. Wong, S. Cherepov, P. K. Amiri, K. Wang, J. Hockel, *et al.*, "Spin wave nanofabric update," in *Proc. Intl. Symp. Nanoscale Architectures* (2012).

[9] P. Shabadi, A. Khitun, K. Wong, P. K. Amiri, K. L. Wang, and C. A. Moritz, "Spin wave functions nanofabric update," in *Nanoscale Architectures (NANOARCH), 2011 IEEE/ACM International Symposium on* (IEEE, 2011) pp. 107–113.

[10] A. Khitun and K. L. Wang, "Non-volatile magnonic logic circuits engineering," Journal of Applied Physics **110**, 034306 (2011).

[11] S. Cherepov, P. K. Amiri, J. G. Alzate, K. Wong, M. Lewis, P. Upadhyaya, J. Nath, M. Bao, A. Bur, T. Wu, *et al.*, "Electric-field-induced spin wave generation using multiferroic magnetoelectric cells," Applied Physics Letters **104**, 082403 (2014).

[12] S. Dutta, D. Nikonov, S. Manipatruni, I. Young, and A. Naeemi, "Spice circuit modeling of pma spin wave bus excited using magnetoelectric effect," (2014).

[13] S. Dutta, S.-C. Chang, N. Kani, D. E. Nikonov, S. Manipatruni, I. A. Young, and A. Naeemi, "Non-volatile clocked spin wave interconnect for beyond-cmos nanomagnet pipelines," Scientific Reports **5** (2015).

[14] W. F. Brown Jr, "Thermal fluctuations of a single-domain particle," Journal of Applied Physics **34**, 1319–1320 (1963).

[15] S. Manipatruni, D. E. Nikonov, and I. A. Young, "Modeling and design of spintronic integrated circuits," Circuits and Systems I: Regular Papers, IEEE Transactions on **59**, 2801–2814 (2012).

[16] L. Liu, T. Moriyama, D. Ralph, and R. Buhrman, "Reduction of the spin-torque critical current by partially canceling the free layer demagnetization field," Applied Physics Letters **94**, 122508 (2009).

[17] M. Beleggia, M. De Graef, and Y. Millev, "The equivalent ellipsoid of a magnetized body," Journal of Physics D: Applied Physics **39**, 891 (2006).

[18] G. Daalderop, P. Kelly, and F. Den Broeder, "Prediction and confirmation of perpendicular magnetic anisotropy in co/ni multilayers," Physical review letters **68**, 682 (1992).

[19] T. A. Nguyen, Y. Fang, V. Fallahi, N. Benatmane, S. Mohseni, R. Dumas, and J. Åkerman, "[co/pd]–nife exchange springs with tunable magnetization tilt angle," Applied Physics Letters **98**, 172502 (2011).

[20] M. d'Aquino, C. Serpico, G. Coppola, I. Mayergoyz, and G. Bertotti, "Midpoint numerical technique for stochastic landau-lifshitz-gilbert dynamics," Journal of applied physics **99**, 08B905 (2006).

[21] D. Pinna, D. L. Stein, and A. D. Kent, "Spin-torque oscillators with thermal noise: A constant energy orbit approach," Physical Review B **90**, 174405 (2014).

[22] I. D. Mayergoyz, G. Bertotti, and C. Serpico, *Nonlinear magnetization dynamics in nanosystems* (Elsevier, 2009).

[23] M. J. Donahue and D. G. Porter, *OOMMF User's guide* (US Department of Commerce, Technology Administration, National Institute of Standards and Technology, 1999).

[24] J.-M. Hu and C. Nan, "Electric-field-induced magnetic easy-axis reorientation in ferromagnetic/ferroelectric layered heterostructures," Physical Review B **80**, 224416 (2009).

[25] K. Roy, S. Bandyopadhyay, and J. Atulasimha, "Switching dynamics of a magnetostrictive single-domain nanomagnet subjected to stress," Physical Review B **83**, 224412 (2011).